Pergamon

Int. J. Heat Mass Transfer. Vol. 37, No. 15, pp. 2327–2342, 1994

0017–9310/94 $7.00+0.00

0017–9310(93)E0121–V

Plane-parallel advective binary mixture flow stability in a horizontal layer

G. Z. GERSHUNI and A. V. SHALIMOV
Department of Theoretical Physics, Perm State University, 614600 Perm, Russia

and

V. M. MYZNIKOV
Department of General Physics, Perm State Pedagogical Institute, 614600 Perm, Russia

(*Received* 16 *March* 1993)

Abstract—The stability of a plane-parallel stationary advective binary mixture flow in a horizontal layer due to horizontal temperature and concentration gradients is investigated theoretically. The layer surfaces are assumed rigid. The main plane-parallel flow and its linear stability against small two-dimensional disturbances is studied with three types of boundary conditions for temperature and concentration: (a) fixed longitudinal temperature and concentration gradients; (b) a constant longitudinal temperature gradient and impermeability; and (c) heat insulation and impermeability. The spectral problem for the amplitudes of normal perturbations is formulated. The case of mechanical equilibrium in the absence of a density gradient is considered. Further, the case of long wave instability for (b) and (c) is studied analytically by an asymptotic expansions technique. The results of numerical simulation of a complete spectral problem for amplitudes are discussed for $Pr = 0.01$ and $Sc \geqslant Pr$. The limits of the flow stability and the characteristics of critical perturbations are determined for all the indicated types of boundary conditions. The instability is shown to be caused by hydrodynamic and thermoconcentration (double diffusive) mechanisms.

1. INTRODUCTION

FOR THE past 20 years many research workers have been interested in advective flows arising in liquids and gases in the gravitational field due to a horizontal density gradient. This interest is dictated by a number of geophysical and technological applications, which in particular include the atmospheric Hadley circulation, some types of motion in the ocean and in the Earth's crust and mantle, transfer processes in shallow water reservoirs, motion of the melt in crystal growth installations (the horizontal variant of Bridgeman technique), and so on.

As velocity increases, advective flows lose their stability being naturally accompanied by the crisis of heat and mass transfer. A review of the stability examination results of single component liquid advective flows in a plane horizontal layer with a longitudinal horizontal temperature gradient is given in refs. [1, 2]. A remarkable feature of advective flows is the existence of instability mechanisms, which are different by their physical nature, but which eventually lead to the main flow crisis in various ranges of governing parameters. For instance, when the Prandtl number, Pr, is small, the purely hydrodynamic instability mechanism underlying the interaction of advective flows travelling in opposite directions is of great significance. For moderate and large Prandtl numbers, instability is, as a rule, caused by the stratification (Rayleigh) mechanism operating in those cases when flow leads to the formation of zones of potentially unstable stratification in the layer. The region of potentially stable stratification can also give rise to growing disturbances connected by their nature with the generation of internal waves; the corresponding instability mechanism, just as the hydrodynamic one, operates in the range of small Pr numbers. Finally, if there is a free surface, the appearance of the specific Marangoni instability mechanism is possible which arises due to the thermocapillary effect.

Investigations of flow structure and of heat and mass transfer in crystal growth installations for the horizontal variant of directed crystallization technique [3, 4], as well as geophysical applications, naturally require the extension of the advective flow stability problem to the cases of binary and multicomponent mixtures. Apart from the instability mechanisms operative in a single component medium, the mixture can be expected to display various manifestations of thermoconcentration (double diffusive) instability mechanism due to the difference in characteristic times for heat and mass diffusion.

The problem of plane-parallel advective binary mixture flow instability has received comparatively little attention [5–7]. In refs. [5, 6] the binary mixture flow in a layer with rigid heat insulated boundaries was considered in the presence of a horizontal temperature gradient and at different (fixed) concentrations cor-

NOMENCLATURE

A longitudinal temperature gradient
B longitudinal concentration gradient
C concentration
$c_0(y)$ concentration profile in basic flow
D diffusivity
$\mathfrak{D}$ operator $d^2/dy^2 - k^2$
$(f_1(y), f_2(y), f_3(y))$ functions determining basic profiles
g acceleration of gravity
Gr thermal Grashof number
Gr_d concentrational Grashof number
Gr_m thermal Grashof number minimized with respect to k
h half of layer thickness
k wavenumber
k_m critical wavenumber
p pressure
Pr Prandtl number
Pr_* limiting Prandtl number for hydrodynamic mode
Ra thermal Rayleigh number
Ra_d concentrational Rayleigh number
$\tilde{R}$, R_c stability parameter for mechanical equilibrium and its critical value
S Lewis number
Sc Schmidt number
T temperature
t time
v velocity
$v_0(y)$ velocity profile in basic flow
(v', p', T', C') small disturbances of velocity, pressure, temperature, and concentration
(x, y, z) Cartesian coordinates.

Greek symbols
β_1 coefficient of thermal expansion
β_2 concentrational coefficient of density
γ unit vector directed vertically upward
ζ disturbance in the case of equilibrium
$\lambda = \lambda_r + i\lambda_i$ characteristic decrement
ν coefficient of kinematic viscosity
ρ density
ρ_0 standard value of density
$\tau_0(y)$ temperature profile in basic flow
χ coefficient of thermal diffusivity
Ψ stream function
(ψ, η) amplitudes conjugated to (ϕ, ζ)
$(\phi(y), \theta(y), \xi(y))$ disturbance amplitudes for stream function, temperature, and concentration.

responding to unstable vertical stratification. In ref. [7] the case of a binary mixture is discussed for a layer bounded by rigid impermeable highly conducting surfaces in the presence of both longitudinal temperature and concentration gradients. It is shown that three instability mechanisms are realized in the mixture which are typical for a single component medium and which are associated with the development of plane and helical disturbances.

In this paper we begin a systematic study of linear plane-parallel binary mixture advective flow stability in a plane horizontal layer bounded by rigid surfaces in the presence of longitudinal temperature and concentration gradients. The main flow and its stability against normal two-dimensional monotonous perturbations are investigated for three types of boundary conditions: (a) fixed longitudinal temperature and concentration gradients; (b) impermeability and constant longitudinal temperature gradient; (c) impermeability and thermal insulation. The spectral amplitude problem is formulated for the case of two-dimensional normal disturbances. It is expected that for (b) and (c), long-wave perturbations will be of importance. For their description, the regular perturbation technique is used based on the series expansions of amplitudes and eigenvalue (decrement) in powers of a small parameter, i.e. the wavenumber k. To solve the problem at arbitrary (finite) values of k, numerical techniques are used. First, a special case of mechanical equilibrium is considered which appears under the conditions of mutual compensation of density gradients produced by horizontal temperature and concentration gradients; here the instability originates which is caused by thermoconcentration mechanism. Numerical solution of the complete spectral amplitude problem is carried out for the Prandtl number $Pr = 0.01$ at the Schmidt number $Sc \geqslant Pr$ (corresponding to molten metal or an admixture-containing semiconductor). The boundary of the steady-state flow stability is described by a curve in the plane of the thermal Grashof number, Gr, vs the concentrational Grashof number, Gr_d. This curve (at fixed Pr) depends on the Schmidt number, Sc. Such families of stability curves are plotted for all the mentioned types of boundary conditions. The critical values of the wavenumber have been determined and the forms of critical disturbances have been studied. The numerical results make it possible to provide explanations for details relating to the interaction of hydrodynamic and thermoconcentrational instability mechanisms.

Section 2 presents the formulation of the problem, including governing equations, and introduces the dimensionless variables and similarity criteria. Solutions describing the plane-parallel advective regime for all indicated types of boundary conditions are given in Section 3. Section 4 contains the stability problem and spectral amplitude problem formu-

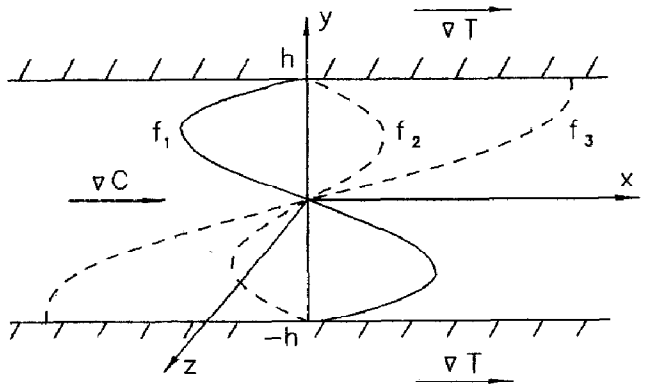

FIG. 1. Coordinate system, profiles of functions f_1, f_2, f_3.

lations. The description of the technique applied to solving the spectral amplitude problem is given in Section 5. Section 6 deals with the results of solution of the equilibrium stability problem. Section 7 includes the long-wave instability analysis for (b) and (c) variants. Sections 8 and 9 contain the discussion of numerical results for stability boundaries and critical perturbations characteristics.

2. THE PROBLEM FORMULATION. BASIC EQUATIONS

Consider an infinite plane horizontal layer of binary mixture between two parallel plates $y = \pm h$ (Fig. 1). In the interior of the layer constant longitudinal gradients of temperature and concentration of the lightest component of the mixture are maintained:

$$\lim_{L\to\infty}\frac{1}{2L}\int_{-L}^{+L}\frac{\partial T}{\partial x}\,dx = A \tag{1}$$

$$\lim_{L\to\infty}\frac{1}{2L}\int_{-L}^{+L}\frac{\partial C}{\partial x}\,dx = B. \tag{2}$$

The objective is to determine a steady-state advective flow originating under the above conditions and to study its stability against small disturbances.

Suppose that the deviations of temperature T and concentration C from some standard values are small, and that the mixture density depends linearly on these deviations:

$$\rho = \rho_0(1-\beta_1 T-\beta_2 C).$$

Here ρ_0 is the density corresponding to standard temperature and concentration, β_1 is the coefficient of thermal expansion, β_2 is the concentrational coefficient of density (it is supposed that $\beta_2 > 0$ because C is the concentration of the lightest component of the mixture).

Let us write the equations of binary mixture convection in Boussinesq approximation (see ref. [8]). Assuming all the transport coefficients to be independent of temperature, concentration and pressure and neglecting the 'cross'-effects of thermodiffusion and diffusional heat conduction, we obtain a system of equations

$$\frac{\partial \upsilon}{\partial t}+(\upsilon\nabla)\upsilon = -\frac{1}{\rho_0}\nabla p+\nu\Delta\upsilon+g(\beta_1 T+\beta_2 C)\gamma$$

$$\operatorname{div}\upsilon = 0$$

$$\frac{\partial T}{\partial t}+\upsilon\nabla T = \chi\Delta T$$

$$\frac{\partial C}{\partial t}+\upsilon\nabla C = D\Delta C. \tag{3}$$

Here υ is the velocity, p is the pressure deviation from the hydrostatic one, corresponding to constant density ρ_0; ν, χ, D are the coefficients of kinematic viscosity, thermal diffusivity and of diffusion respectively; g is the gravity acceleration; γ is the unit-vector directed vertically upward.

The system of equations (3) can be written in non-dimensional form. Introduce the following units for distance, time, velocity, temperature, concentration, and pressure: h, h^2/ν, ν/h, Ah, Bh, $\rho_0\nu^2/h^2$, respectively. Then, the equations will acquire the form

$$\frac{\partial \upsilon}{\partial t}+(\upsilon\nabla)\upsilon = -\nabla p+\Delta\upsilon+(Gr\cdot T+Gr_d\cdot C)\gamma,$$

$$\operatorname{div}\upsilon = 0$$

$$\frac{\partial T}{\partial t}+\upsilon\nabla T = \frac{1}{Pr}\Delta T$$

$$\frac{\partial C}{\partial t}+\upsilon\nabla C = \frac{1}{Sc}\Delta C. \tag{4}$$

The system of equations (4) contains four non-dimensional parameters: thermal and concentrational Grashof numbers based on longitudinal temperature and concentration gradients, Gr and Gr_d, and also the Prandtl number Pr and Schmidt number Sc:

$$Gr = \frac{g\beta_1 Ah^4}{\nu^2},\quad Gr_d = \frac{g\beta_2 Bh^4}{\nu^2},\quad Pr = \frac{\nu}{\chi},\quad Sc = \frac{\nu}{D}. \tag{5}$$

Hereafter, we will use also the thermal and concentrational Rayleigh numbers, i.e. Ra and Ra_d. In some cases, one other parameter, i.e. the Lewis number, S, determining the relation between characteristic times for diffusion and heat conduction, plays an important role. These parameters are defined as follows:

$$Ra = \frac{g\beta_1 Ah^4}{\nu\chi} = Gr\cdot Pr,$$

$$Ra_d = \frac{g\beta_2 Bh^4}{\nu D} = Gr\cdot Sc,\quad S = \frac{D}{\chi} = \frac{Pr}{Sc}. \tag{6}$$

3. BASIC FLOW

The system of equations (4) has a solution which describes a steady-state plane-parallel advective flow

appearing in a horizontal layer under the action of longitudinal temperature and concentration gradients. This flow has the following structure

$$v_{0y} = v_{0z} = 0, \quad v_{0x} = v_0(y), \quad p_0 = p_0(x, y)$$
$$T_0 = x + \tau_0(y), \quad C_0 = x + c_0(y), \tag{7}$$

where v_0, p_0, τ_0, and c_0 are the solutions of the equations

$$\frac{\partial p_0}{\partial x} = v_0'', \qquad \frac{\partial p_0}{\partial y} = Gr \cdot T_0 + Gr_d \cdot C_0 \tag{8}$$

$$\frac{1}{Pr}\tau_0'' = v_0, \qquad \frac{1}{Sc}c_0'' = v_0. \tag{9}$$

Equations (8) yields

$$v_0''' = Gr + Gr_d. \tag{10}$$

Suppose that the layer boundaries are rigid, so that the non-sleep condition is satisfied on them. Besides, suppose that the flow is 'closed', i.e. the total flux through the section of the layer is equal to zero. Thus we have

$$v_0(\pm 1) = 0, \qquad \int_{-1}^{+1} v_0(y)\,dy = 0. \tag{11}$$

Performing integration of equations (10) taking into account equation (11) we obtain (irrespective of the boundary conditions for temperature and concentration) the velocity distribution in the plane-parallel advective flow

$$v_0 = (Gr + Gr_d) f_1(y), \qquad f_1(y) = \tfrac{1}{6}(y^3 - y). \tag{12}$$

The temperature and concentration profiles are to be determined from equations (9). Hereafter we will consider three variants of boundary conditions:

- variant (a): constant temperature and concentration gradients are maintained on the boundaries of the layer;
- variant (b): constant temperature gradient is maintained on the boundaries and they are impermeable; and
- variant (c): the boundaries of the layer are impermeable and thermally insulated.

We have the following boundary conditions, respectively:

$$y = \pm 1: \quad \tau_0 = c_0 = 0 \tag{13a}$$
$$y = \pm 1: \quad \tau_0 = 0, \quad c_0' = 0 \tag{13b}$$
$$y = \pm 1: \quad \tau_0' = c_0' = 0. \tag{13c}$$

Integration of equations (9) subject to conditions (13) yields the temperature and concentration profiles for the three variants of the boundary conditions

$$\tau_0 = Pr(Gr + Gr_d) f_2(y), \quad c_0 = Sc(Gr + Gr_d) f_2(y),$$
$$f_2(y) = \frac{1}{360}(3y^5 - 10y^3 + 7y) \tag{14a}$$

$$\tau_0 = Pr(Gr + Gr_d) f_2(y), \quad c_0 = Sc(Gr + Gr_d) f_3(y),$$
$$f_3(y) = \frac{1}{360}(3y^5 - 10y^3 + 15y) \tag{14b}$$

$$\tau_0 = Pr(Gr + Gr_d) f_3(y), \quad c_0 = Sc(Gr + Gr_d) f_3(y). \tag{14c}$$

The solution presented extends the well-known Birikh solution [9] to the case of plane-parallel binary mixture advection. The functions $f_1(y)$, $f_2(y)$, and $f_3(y)$ which determine the velocity, temperature, and concentration profiles for different variants of boundary conditions are shown schematically in Fig. 1. The velocity profile described by the third-degree polynomial (12) corresponds to the existence of two counter-flows and has an inflection point. Thus, it is evident that, irrespective of boundary conditions for temperature and concentration, it is possible to expect the appearance of the hydrodynamic instability mode of non-viscous nature, which develops as a system of steady vortices on the boundary of two counter-flows (at least, in the region of small Prandtl and Schmidt numbers). The transverse distributions of temperature and concentration testify to the existence of the regions of potentially stable and potentially unstable density stratification in the layer. The position of these regions depends on the relationship between the parameters of the problem; for example, it depends on the signs of Gr and Gr_d. Thus, the appearance of stratificational modes of instability is possible for both Rayleigh type and those caused by the generation of internal waves. Finally, in the situation discussed, a specific thermoconcentrational (double-diffusive) mechanism of instability can appear which is caused by the difference in the characteristic relaxation times for temperature and concentration. As it is seen from equations (12) and (14), when $Gr_d = -Gr$, we obtain $v_0 = 0$, $\tau_0 = 0$ and $c_0 = 0$, i.e. we deal with mechanical equilibrium when the total density gradient is absent, since the horizontal density gradients, caused by the temperature and concentration gradients compensate each other. It is evident that both hydrodynamical and stratificational modes of instability are absent in this situation. As for the thermoconcentrational mode of instability, the situation, on the contrary, is favourable for its development (see ref. [1]). To be sure, the thermoconcentrational mechanism of instability is operative not only in the special case when $Gr + Gr_d = 0$; this situation is outstanding only because two other mechanisms are suppressed.

4. STATEMENT OF STABILITY PROBLEM. EQUATIONS FOR DISTURBANCES

To investigate the stability of the described plane-parallel flows introduce small disturbances and consider disturbed fields:

$$\mathbf{v} = \mathbf{v}_0 + \mathbf{v}', \quad p = p_0 + p',$$
$$T = T_0 + T', \quad C = C_0 + C'. \tag{15}$$

Substituting representation (15) into the basic system of equations (4) and linearizing about the basic solution, equations (7) and (8), we obtain a system of equations for disturbances:

$$\frac{\partial \boldsymbol{v}'}{\partial t}+[(\boldsymbol{v}_0\nabla)\boldsymbol{v}'+(\boldsymbol{v}'\nabla)\boldsymbol{v}_0] = -\nabla p'+\Delta \boldsymbol{v}' + (GrT'+Gr_dC')\gamma \quad \operatorname{div}\boldsymbol{v}' = 0,$$

$$\frac{\partial T'}{\partial t}+\boldsymbol{v}_0\nabla T'+\boldsymbol{v}'\nabla T_0 = \frac{1}{Pr}\Delta T',$$

$$\frac{\partial C'}{\partial t}+\boldsymbol{v}_0\nabla C'+\boldsymbol{v}'\nabla C_0 = \frac{1}{Sc}\Delta C'. \qquad (16)$$

In this work, we shall limit our discussion to two-dimensional (2D) disturbances of the form

$$v_z' = 0, \quad v_x' = v_x'(x,y,t), \quad v_y' = v_y'(x,y,t),$$
$$p' = p'(x,y,t), \quad T' = T'(x,y,t), \quad C' = C'(x,y,t) \qquad (17)$$

and introduce the stream function by relations

$$v_x' = \frac{\partial \Psi}{\partial y}, \qquad v_y' = -\frac{\partial \Psi}{\partial x}. \qquad (18)$$

Considering 2D disturbances, we thus confine our attention only to instability modes caused by the action of hydrodynamic and thermoconcentrational mechanisms [the experience of the stability problem solution for an one-component fluid shows that stratificational instability modes substantially result from 3D spiral-type disturbances (see refs. [1, 2])].

Excluding pressure from equation (16), introducing the stream function and considering the 'normal mode'-type disturbances

$$(\Psi, T', C') = (\phi(y), \theta(y), \xi(y)) \exp(-\lambda t + ikx) \qquad (19)$$

we obtain a system of linear homogeneous ordinary differential equations for the amplitudes ϕ, θ and ξ:

$$(\phi^{IV}-2k^2\phi''+k^4\phi)+ik[v_0''\phi-v_0(\phi''-k^2\phi)] - ik(Gr\theta+Gr_d\xi) = -\lambda(\phi''-k^2\phi)$$

$$\frac{1}{Pr}(\theta''-k^2\theta)+ik(\tau_0'\phi-v_0\theta)-\phi' = -\lambda\theta$$

$$\frac{1}{Sc}(\xi''-k^2\xi)+ik(C_0'\phi-v_0\xi)-\phi' = -\lambda\xi. \qquad (20)$$

Here $\lambda = \lambda_r + i\lambda_i$ is the decrement, k is the wavenumber; here and hereafter the prime means differentiation with respect to the transverse coordinate y.

The boundary conditions for amplitudes for the three variants are of the form

$$y = \pm 1: \quad \phi = \phi' = 0, \quad \theta = 0, \quad \xi = 0 \qquad (21a)$$

$$y = \pm 1: \quad \phi = \phi' = 0, \quad \theta = 0, \quad \xi' = 0 \qquad (21b)$$

$$y = \pm 1: \quad \phi = \phi' = 0, \quad \theta' = 0, \quad \xi' = 0. \qquad (21c)$$

The system of amplitude equations (20) together with one of the variants of boundary conditions (21) form the spectral amplitude problem with the characteristic decrement λ as an eigenvalue; the decrement λ depends on all the parameters Gr, Gr_d, Pr, Sc, and k. The eigenvector of the problem is the set of characteristic amplitudes ϕ, θ, and ξ. If the eigenvalue λ is real, the stability boundary is determined from the condition $\lambda = 0$. If the eigenvalue is complex one, $\lambda = \lambda_r + i\lambda_i$, then the stability boundary can be determined from the condition $\lambda_r = 0$. In this case the imaginary part λ_i does mean the frequency of neutral oscillations. The study of stability thus reduces to the construction of a dispersional relation for problem (20), (21).

Note that physically the situation does not change if a simultaneous change occurs in the signs of Gr and Gr_d, i.e. in the directions of the horizontal temperature and concentration gradients (this also relates to the instability characteristics). It is evident that in the case when the amplitudes θ and ξ satisfy the same boundary conditions [variants (a) and (c)] there also exists symmetry with respect to the changes $\theta \Leftrightarrow \xi$, $Gr \Leftrightarrow Gr_d$, and $Pr \Leftrightarrow Sc$.

5. APPROXIMATE METHODS

It is hardly possible to rely on the obtention of an exact solution for the formulated spectral amplitude problem (20), (21). To solve the problem, we used approximate methods. In the case of impermeable boundaries [variants (b) and (c)], we can postulate that there is a long-wave instability mode which under certain conditions turns out to be most dangerous. To solve the problem for long-wave disturbances, the regular method of perturbations with wavenumber k as a small parameter was used. This allows one to find the stability boundaries for a long-wave mode analytically.

In the case of an arbitrary relation between the parameters, the problem was solved numerically by two methods. In the first place a straightforward numerical integration of the amplitude equation system was employed using the differential factorization procedure (see ref. [9]). Secondly the Galerkin method was used in its version when the systems of characteristic disturbance amplitudes in a motionless layer are used as basic functions.

The eigenfunctions of the following two-point boundary problem were used to approximate the stream-function amplitude

$$\phi_n^{IV}-2k^2\phi_n+k^4\phi_n = -\mu_n(\phi_n''-k^2\phi_n)$$
$$\phi_n(\pm 1) = \phi_n'(\pm 1) = 0, \quad n = 0, 1, 2, \ldots. \qquad (22)$$

To construct approximations for the amplitudes θ and ξ, we used the boundary problems for the basic functions, respectively

$$\theta_n''-k^2\theta^n = -\nu_n Pr\,\theta_n, \quad \theta_n(\pm 1) = 0\,(a), (b); \quad \theta_n'(\pm 1) = 0\,(c) \qquad (23)$$

$$\xi_n'' - k^2\xi_n = -\chi_n Sc\,\xi_n, \quad \xi_n(\pm 1) = 0\,(a);$$
$$\xi_n'(\pm 1) = 0\,(b), (c). \tag{24}$$

In this work, approximations containing totally up to 80 basic functions were used. Such approximations guarantee the internal convergence of the method in the investigated region of parameters. In this region the results received by both methods (the Galerkin method and the method of differential factorization) practically coincide.

6. MECHANICAL EQUILIBRIUM

As already noted, when

$$Gr + Gr_d = 0 \tag{25}$$

the basic plane-parallel flow velocity is equal to zero. Also equal to zero are the parts of temperature and concentration distributions, τ_0 and c_0, that depend on the transverse coordinate. Thus, we deal with the mechanical equilibrium state when the density distribution is homogeneous in space but the horizontal temperature and concentration gradients are not zero and have the opposite directions. In this situation only the thermoconcentrational mechanism of instability is operative. The instability has a monotonous character, and the neutral regime should be determined from the condition $\lambda = 0$. Then, the system of equations (20) yields

$$(\phi^{IV} - 2k^2\phi'' + k^4\phi) - ik(Gr\theta + Gr_d\xi) = 0$$
$$\frac{1}{Pr}(\theta'' - k^2\theta) - \phi' = 0, \quad \frac{1}{Sc}(\xi'' - k^2\xi) - \phi' = 0 \tag{26}$$

with appropriate boundary conditions (21a–c).

First, consider cases (a) and (c) when the amplitudes θ and ξ satisfy the same homogeneous boundary conditions. In this case the second and the third equations of system (26) mean that

$$\frac{\theta}{Pr} = \frac{\xi}{Sc}. \tag{27}$$

Introducing the new variable $\theta/Pr = \xi/Sc = \xi$ and operator $\mathscr{D} = d^2/dy^2 - k^2$, we obtain two spectral problems

$$\mathscr{D}^2\phi - ik(Ra + Ra_d)\zeta = 0, \quad \mathscr{D}\zeta - \phi' = 0$$
$$\phi(\pm 1) = \phi'(\pm 1) = 0, \quad \zeta(\pm 1) = 0\,(a),$$
$$\zeta'(\pm 1) = 0\,(c). \tag{28}$$

It follows from this that the sum $Ra + Ra_d \equiv \tilde{R}$, depending on the wavenumber k, is the critical parameter which determines the equilibrium stability boundary. Numerical solution of the problem for case (a) shows that the critical number $\tilde{R}$ corresponding to the threshold which results from minimization with respect to the wavenumber, is $\tilde{R} \equiv R_c \cong -406.8$; the wavenumber of the most dangerous disturbance is equal to $k_m \cong 1.256$. Taking into account equation (25), we find the parameters on the instability boundary for case (a)

$$Ra_d = -\frac{406.8}{1-S}, \quad Ra = \frac{406.8S}{1-S},$$
$$Gr_d = -\frac{406.8}{Sc(1-S)}, \quad Gr = \frac{406.8}{Sc(1-S)}\left(S = \frac{Pr}{Sc}\right). \tag{29}$$

It is possible to demonstrate that the same results take place in case (c), although here the boundary condition $\zeta(\pm 1) = 0$ must be replaced by $\zeta'(\pm 1) = 0$. We actually write down the spectral problem for case (c)

$$\mathscr{D}^2\phi - ik\tilde{R}\zeta = 0, \quad \mathscr{D}\zeta - \phi' = 0;$$
$$\phi(\pm 1) = \phi'(\pm 1) = \zeta'(\pm 1) = 0. \tag{30}$$

Also, let us write the problem which is conjugate to problem (30). It can be derived from (30) by a standard manner and has the form

$$\mathscr{D}^2\psi + \eta' = 0, \quad \mathscr{D}\eta + ik\tilde{R}\psi = 0;$$
$$\psi(\pm 1) = \psi'(\pm 1) = \eta'(\pm 1) = 0, \tag{31}$$

where (ψ, η) are the amplitudes conjugate to (ϕ, ζ). Problem (31) has the same spectrum of eigenvalues as the basic problem (30). Differentiation of the second equation of system (31) gives

$$\mathscr{D}^2\psi - ik\tilde{R}f = 0, \quad \mathscr{D}f - \psi' = 0;$$
$$\psi(\pm 1) = \psi'(\pm 1) = f(\pm 1) = 0, \tag{32}$$

where f is a new variable determined by the relation $\eta' = -ik\tilde{R}f$. The boundary problem (32) coincides with that for case (a). Thus, both spectral problems (28) have a common spectrum of eigenvalues and the results presented by equations (29) are preserved in case (c). From these results it is seen that there exists absolute stabilization of equilibrium when $S \to 1$. It is evident from the physical point of view: indeed, the thermoconcentrational mechanism of instability is caused by the difference in the relaxation times for diffusion and heat conduction, i.e. by the difference in the Prandtl, Pr, and the Schmidt, Sc, numbers.

In the case of variant (b) the situation is somewhat more complicated since relation (27) is no longer valid because of the difference in the boundary conditions for θ and ξ. Numerical results obtained for different values of $S = Pr/Sc$ show that the wavenumber of the most dangerous disturbance, k_m, depends slightly on S. As in cases (a) and (c) for the critical Ra_d we have the formula $Ra_d = R_c/(1-S)$, where, however, R_c is a function of S. The values of R_c and k_m for different values of the parameter S are listed in Table 1. Comparing the data from Table 1 and these given by equations (29) we see that in the region of small values of S all three variants of boundary conditions give the same result for the instability characteristics Ra_d and k_m.

Table 1. The equilibrium instability parameters for variant (b)

S	$-R_c$	k_m
0	406.84	1.266
0.0001	406.85	1.266
0.0002	406.87	1.266
0.0005	406.90	1.266
0.001	406.96	1.266
0.002	407.08	1.266
0.005	407.44	1.268
0.01	408.05	1.268
0.02	409.32	1.272
0.05	413.49	1.282
0.1	421.95	1.302
0.2	447.14	1.368
0.5	728.52	2.068

7. LONG-WAVE INSTABILITY

In the cases of impermeable boundaries of the layer [variants (b) and (c) of boundary conditions] it is possible to expect the existence of long-wave instability with $k_m = 0$ (physically this means that the disturbance wavelength is much larger than the layer thickness). Then to determine the stability boundaries it is possible to apply the regular method of perturbations with the wavenumber k as a small parameter.

Consider variant (b) of boundary conditions when $\theta(\pm 1) = 0$, and $\xi'(\pm 1) = 0$ and let $k = 0$ in general equations (20). This yields zero-order equations

$$\phi_0^{IV} = -\lambda_0 \phi_0''$$

$$\frac{1}{Pr}\theta_0'' - \phi_0' = -\lambda_0 \theta_0$$

$$\frac{1}{Sc}\xi_0'' - \phi_0' = -\lambda_0 \xi_0 \qquad (33)$$

with boundary conditions $\theta_0(\pm 1) = 0$ and $\xi'(\pm 1) = 0$. It can be shown that all the levels of the spectrum of this problem correspond to damping disturbances except for one which is a neutral 'concentrational-type' level:

$$\lambda_0 = 0, \quad \phi_0 = 0, \quad \theta_0 = 0, \quad \xi_0 = \text{const}. \qquad (34)$$

Here the constant can be chosen to be equal to unity, for example, under appropriate normalization.

When k is small the solution can be constructed in the form of power expansions

$$\phi = \phi_1 k + \phi_2 k^2 + \dots$$

$$\theta = \theta_1 k + \theta_2 k^2 + \dots$$

$$\xi = \xi_0 + \xi_1 k + \xi_2 k^2 + \dots$$

$$\lambda = \lambda_1 k + \lambda_2 k^2 + \dots. \qquad (35)$$

Substituting these expansions into the original system of amplitude equations (20) and equating the terms at the same degrees of k, we obtain the systems of successive approximations: in the first order

$$\phi_1^{IV} = iGr_d \xi_0$$

$$\frac{1}{Pr}\theta_1'' - \phi_1' = 0$$

$$\frac{1}{Sc}\xi_1'' - \phi_1' = i\xi_0 v_0 - \lambda_1 \xi_0 \qquad (36)$$

in the second order

$$\phi_2^{IV} = -i(v_0''\phi_1 - v_0\phi_1'') + i(Gr\theta_1 + Gr_d\xi_1) - \lambda_1\phi_1''$$

$$\frac{1}{Pr}\theta_2'' - \phi_2' = -i(\tau_0'\phi_1 - v_0\theta_1) - \lambda_1\theta_1$$

$$\frac{1}{Sc}\xi_2'' - \phi_2' = \frac{1}{Sc}\xi_0 - i(c_0'\phi_1 - v_0\xi_1) - \lambda_1\xi_1 - \lambda_2\xi_0 \qquad (37)$$

and so on.

The boundary conditions for amplitudes in successive approximations coincide with those for the total amplitudes. In each order we obtain a non-homogeneous system of equations. The solvability condition allows as to find a relation for appropriate approximation of the characteristic decrement λ.

Let us now turn to the first approximation. The solvability condition can be obtained by integrating both sides of the third equation of system (36) over the layer thickness. Taking into account the boundary conditions and the fact that v_0 is an odd function of y we obtain $\lambda_1 = 0$. Then the solution of system (36) can be written as

$$\phi_1 = i\xi_0 Gr_d(y^2-1)^2/24$$

$$\theta_1 = i\xi_0 PrGr_d(3y^5 - 10y^3 + 7y)/360$$

$$\xi_1 = i\xi_0 Sc\,(Gr + 2Gr_d)\,(3y^5 - 10y^3 + 15y)/360. \qquad (38)$$

The solvability conditions for the second-order equations can be obtained by integrating both sides of the last equation of system (37). A formula for λ_2 is defined as

$$\lambda_2 = \frac{1}{Sc} - \frac{i}{\xi_0}\int_{-1}^{+1}(c_0'\phi_1 - v_0\xi_1)\,dy. \qquad (39)$$

Substituting ϕ_1 and ξ_1 from equations (38) yields

$$\lambda_2 = \frac{1}{Sc} + \frac{2}{2835}Sc(Gr + Gr_d)\,(Gr + 3Gr_d). \qquad (40)$$

The stability boundary can be obtained from the condition $\lambda_2 = 0$. Thus, the equation for the stability boundary on the plane (Gr_d, Gr) will have the form

$$Gr = -2Gr_d \pm \sqrt{Gr_d^2 - \frac{2835}{2Sc^2}} \qquad (41)$$

As can be seen, the neutral line on the plane (Gr_d, Gr) that separates the regions of stability and instability depends only on the parameter Sc but does not depend on Pr. Examples of neutral lines are presented in Fig.

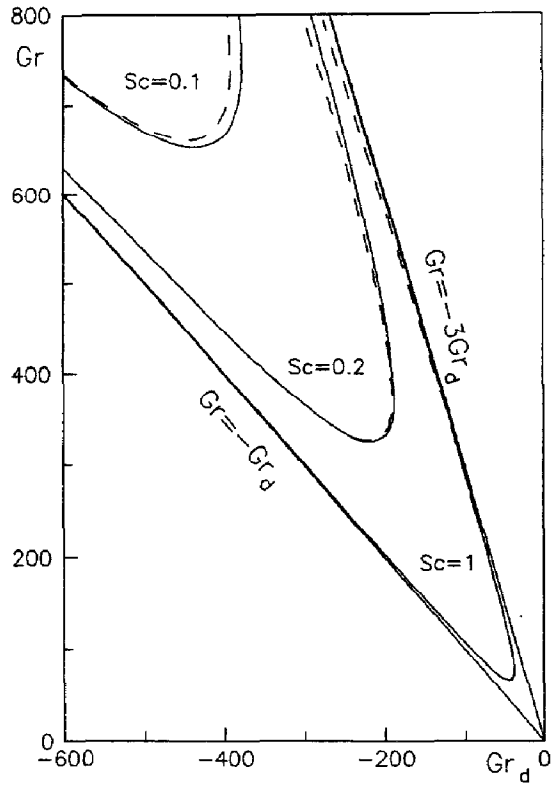

FIG. 2. Stability boundary for long-wave mode on the plane (Gr_d, Gr). Solid line, variant (b); dashed line, variant (c) ($Pr = 0.01$).

2. The long-wave type instability exists only in the case when the signs of Gr_d and Gr are opposite (i.e. if the horizontal gradients of temperature and concentration of the lightest component have opposite directions). The instability region exists if $|Gr_d| > 37.65/Sc$, i.e. $|Ra_d| > 37.65$. The straight lines $Gr = -Gr_d$ (isoline of equilibrium states) and $Gr = -3Gr_d$ are the asymptotes for neutral lines of long-wave disturbances.

In an analogous way one can analyse the case (c) when $\theta'(\pm 1) = 0$ and $\xi'(\pm 1) = 0$. In the zeroth order in k we have

$$\lambda_0 = 0, \quad \phi_0 = 0, \quad \theta_0 = \text{const}, \quad \xi_0 = \text{const}. \quad (42)$$

Constructing the expansions in powers of k and determining corrections of successive orders to characteristic decrement $\lambda_1, \lambda_2, \ldots$ from the solvability conditions we find that $\lambda_1 = 0$, as in the case of variant (b). The solvability condition for the second-order system gives λ_2, and then we find the equation of neutral line on the plane (Gr_d, Gr) from the condition $\lambda_2 = 0$

$$\frac{4}{945} Pr^2 Sc^2 (Gr + Gr_d)^4 + 2(Pr^2 + Sc^2)(Gr + Gr_d)^2 + 4(Gr + Gr_d)(Pr^2 Gr + Sc^2 Gr_d) + 2835 = 0. \quad (43)$$

Now, the neutral lines of long-wave instability depend on both parameters: the Prandtl number, Pr, and the Schmidt number, Sc. The form of the neutral line is qualitatively close to that which corresponds to variant (b) (see Fig. 2). In the limiting case of $Pr \ll 1$, equation (43) reduces to equation (41). The lower branches have the straight line of equilibrium $Gr + Gr_d = 0$ as an asymptote.

The stability boundaries, equations (41) and (43), obtained in this section correspond to the long-wave mode $k = 0$. To find out whether this mode is most dangerous or not, it is necessary to compare with numerical results obtained for the case of an arbitrary k.

8. NUMERICAL RESULTS: VARIANT (a)

Now consider the results of numerical solution of the spectral amplitude problem. Here we shall confine ourselves to the region of small Prandtl numbers, Pr, considering liquid metals or semiconductors with admixtures.

In the case of a single-component medium ($Gr_d = 0$, $Sc = 0$) the instability of advective flow in the region of small Prandtl numbers is caused by a purely hydrodynamic mechanism. If $Pr = 0$, the general amplitude problem reduces to that of Orr–Sommerfeld for the stability of an isothermal flow with a cubic velocity profile, equation (12), and without convective buoyancy force. In this case the minimum of the neutral curve is connected with the wave number $k_m = 1.34$ and corresponds to the critical Grashof number $Gr_m = 495.6$ (see ref. [1]). When the Prandtl number increases, the stability boundary rises sharply due to the formation of the layer of stable stratification just in the region of the development of disturbances. When $Pr \to Pr_*$, the flow becomes absolutely stable respect to hydrodynamic mode. The value of Pr_* depends on the boundary conditions for temperature. For the cases of high-conductive and thermally insulated boundaries we have $Pr_* \cong 0.32$ and $Pr_* \cong 0.15$, respectively (Fig. 3). Just the same results are obtained in the limiting case of an isothermal binary mixture in the absence of a longitudinal temperature gradient when the flow is caused only by a longitudinal concentration gradient ($Gr = 0$, $Pr = 0$). In this case the stability curves correspond to those presented in Fig. 3 but with coordinates $Sc - Gr_{dm}$.

In the general case of binary mixture advection in the presence of both temperature and concentration gradients, the stability boundary is determined by the curve on the plane (Gr_d, Gr), which depends on two parameters; the Prandtl number, Pr, and the Schmidt number, Sc.

In Fig. 4 a family of stability curves on the plane (Gr_d, Gr) is presented (result of minimization respect to the wavenumber k) for $Pr = 0.01$ and several values of $Sc \geqslant Pr$ [variant (a) of the boundary conditions for temperature and concentration]. By symmetry arguments, there is exactly the same family of curves on the plane (Gr_d, Gr) which can be obtained from the family presented in Fig. 4 by inversion through the coordinate origin. For all the stability curves the ori-

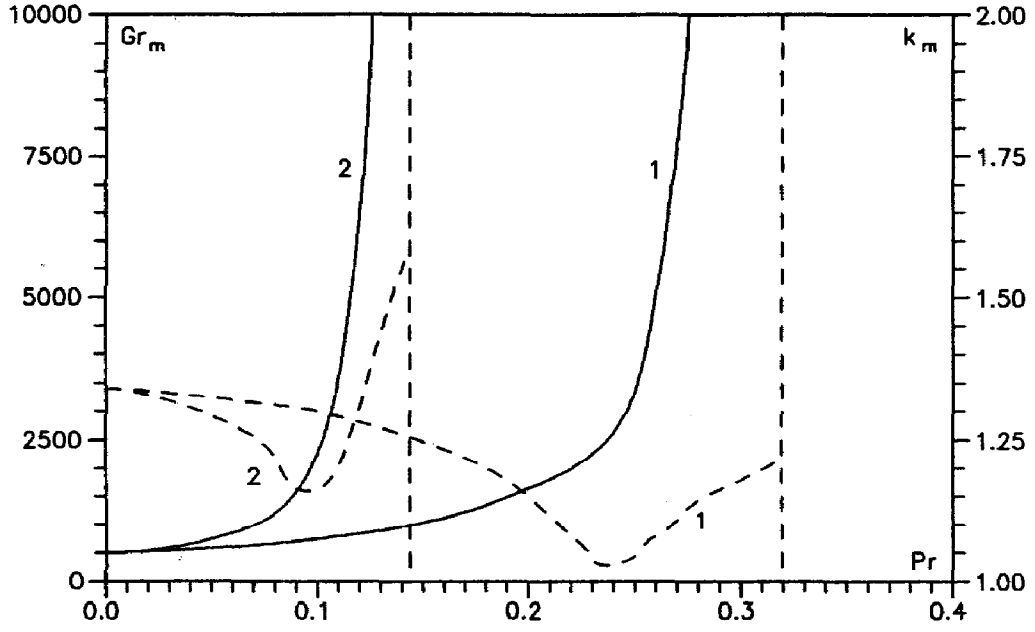

FIG. 3. Stability threshold relative to hydrodynamic mode for a single-component medium. (1) boundaries of high conductivity; (2) thermally insulating boundaries. Solid curves, critical Grashof numbers; dashed curves, critical wavenumbers.

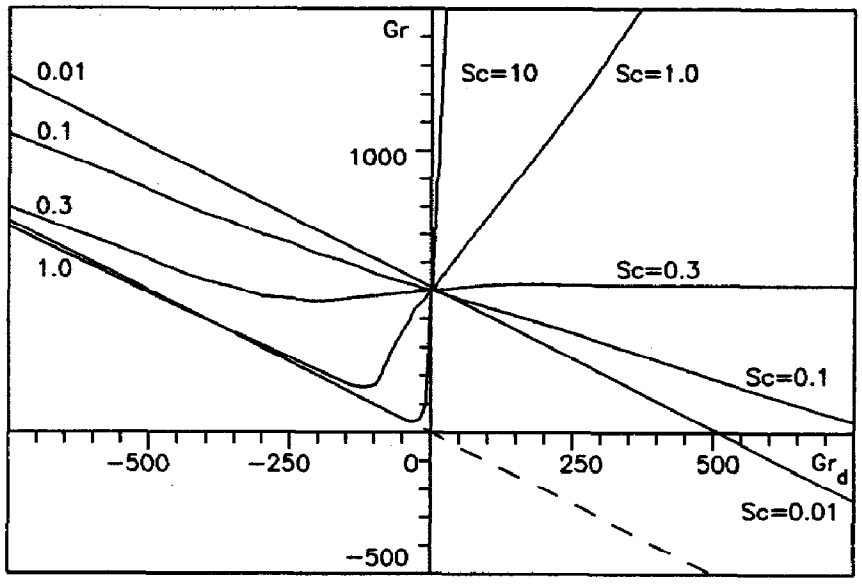

FIG. 4. Stability curves on the plane (Gr_d, Gr) for several values of Sc [$Pr = 0.01$; variant (a)]. Dashed straight line, line of equilibrium: $Gr_d + Gr = 0$.

gin of the coordinates belongs to the region of stability.

Calculations show that, in the investigated region of parameters, the instability has a monotonous character, i.e. the imaginary part of the decrement λ_i is equal to zero on the stability boundary.

As can be seen from amplitude problem (20), (21), in the limiting case of $Pr \ll Pr_*$ and $Sc \ll Sc_*$ it is possible to neglect temperature and concentration disturbances and thus to reduce the problem to the Orr–Sommerfeld problem for velocity distribution (12). Here, the sum $Gr + Gr_d$ will play the role of the instability parameter, and the stability boundary on the plane (Gr_d, Gr) will be described by the straight line $Gr_d + Gr = \text{const}$, where const ≈ 500. The line of the family in Fig. 4 for $Sc = 0.01$ corresponds to this straight line. As Sc increases, the stability curves deform strongly due to the interaction between hydrodynamic and thermoconcentrational mechanisms of instability. All the curves intersect at the point $Gr_d = 0$, $Gr \approx 500$ due to the fixed value of the Prandtl number ($Pr = 0.01$). When $Sc = 0.1$, the point of intersection of the stability curve with the Gr_d axis is displaced to the side of high values of Gr_d in the region $Gr_d > 0$ (as compared to the case of $Sc = 0.01$). The threshold of instability caused by the concentrational

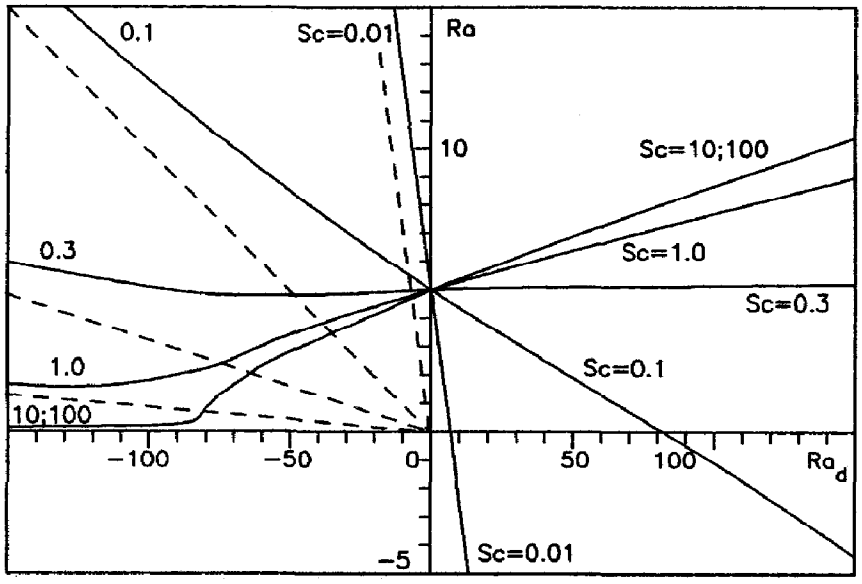

FIG. 5. Stability curves on the plane (Ra_d, Ra) [$Pr = 0.01$; variant (a)]. Dashed straight lines, equilibrium lines for corresponding S: $Ra + S \cdot Ra_d = 0$.

component of the flow rises and when $Sc > Sc_* = 0.32$ the stability curve does not intersect the Gr_d axis. In the region $Gr_d < 0$, the curve of $Sc = 0.1$ intersects the straight line $Gr_d + Gr = 0$, which corresponds to the equilibrium (dashed line in Fig. 4) at the point determined by formula (29), namely, $Gr_d = -406.8/Pr(1-S) = -45.2 \times 10^3$. Thus, in the region of negative and rather large absolute values of Gr_d the instability is transferred to the thermoconcentrational (double-diffusive) mechanism.

With a further increase in Sc (curves $Sc = 1$ and $Sc = 10$), it is possible to distinguish two branches on the stability curve (to the right and to the left of the minimum point) that correspond to physically different instability mechanisms. The increase of stability in the region of positive Gr_d with increasing Gr_d and Sc is caused by the rise of the potentially stable vertical density gradient in the zone of the evolution of disturbances due to the vertical concentration gradient. This part of the stability curve is associated with the hydrodynamical mechanism. The left branch of stability curve, which is very close to the equilibrium line, is associated with the thermoconcentrational instability mechanism.

The behaviour of the family curves in Fig. 4 allows us to predict the asymptotics of the stability boundaries on the (Gr_d, Gr) plane in the limiting case of large Sc. Indeed, in this case the region of instability is bounded by the Gr axis and straight line of equilibrium $Gr + Gr_d = 0$. On the whole this situation persists with variation of the Prandtl number, at least within $0 < Pr < Pr_* = 0.32$, since then the point of intersection of the family curves shifts with the Gr axis. The establishment of asymptotics with increase in Sc can be distinctly seen in Fig. 5 where the stability curves are presented in the coordinates (Ra_d, Ra).

In Fig. 6 a family of neutral curves $Gr(k)$ for $Pr = 0.01$ and $Sc = 1$, and few negative values of Gr_d is presented as an example. Figure 7 includes some numerical data on the wavenumber k_m for the most dangerous disturbances.

It should be emphasized in conclusion to this section that, as numerical results show, in the region of parameters studied, there is no 'factorization' of instability boundaries caused by different mechanisms (now we are dealing only with 2D disturbances). The change of instability mechanisms (i.e. the transition from the hydrodynamical to thermoconcentrational mechanism) takes place continuously along the single stability curve with variation of parameters.

9. NUMERICAL RESULTS: VARIANTS (b) AND (c)

Now consider the results of numerical solution of the problem corresponding to variants (b) and (c) of boundary conditions. As in the previous section, we confine our attention to the cases of $Pr = 0.01$ and $Sc \geqslant Pr$. As compared with variant (a), we see here a qualitatively new factor which is the appearance of long-wave instability. Thus, it is necessary to study the relationship between the long-wave ($k_m = 0$) and cellular ($k_m \neq 0$) modes.

Let us turn to variant (b) and consider as an example the stability boundaries with respect to long-wave and cellular disturbances for the case of $Sc = 0.1$. In the region of $Gr_d > 0$, where the instability is caused by hydrodynamical mechanism, the flow crisis is associated with the cellular mode ($k_m \neq 0$), whereas, for $Gr_d < 0$, where the transition to thermoconcentrational mechanism takes place, there is a characteristic competition between cellular and long-

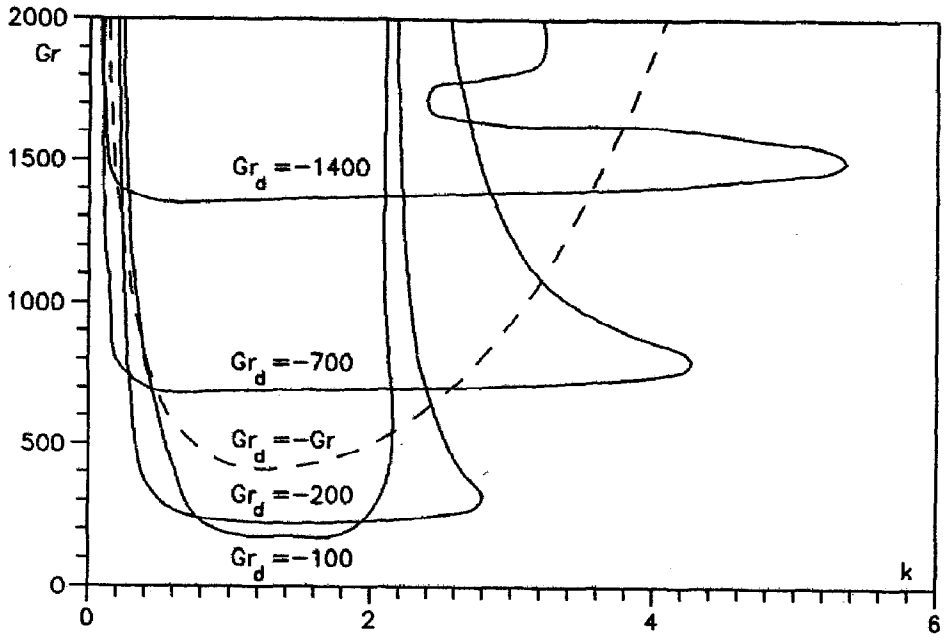

FIG. 6. Neutral curves on the plane (k, Gr) [$Pr = 0.01$; $Sc = 1$; variant (a)]. Dashed curve corresponds to equilibrium : $Gr_d = -Gr$.

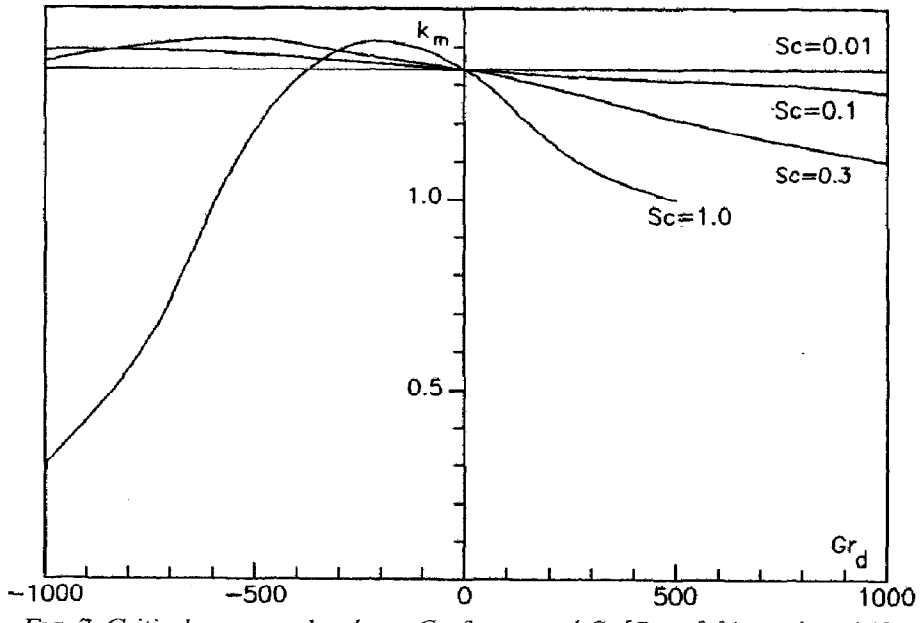

FIG. 7. Critical wavenumber k_m vs Gr_d for several Sc [$Pr = 0.01$; variant (a)].

wave modes. The situation can be illustrated by a family of neutral curves (Fig. 8) and by the stability boundaries on the plane (Gr_d, Gr) (Fig. 9). As can be seen from the form of neutral curve on the plane (k, Gr), at $Gr_d = -100$ the cellular type of instability is distinctly expressed. As $|Gr_d|$ increases, the determination of neutral curves testifies to the origination of the region of long-wave instability. This occurs at $Gr_d = -37.65/Sc = -376.5$ in accordance with formula (41). It can be seen that at $Gr_d = -377$ and -400 there are regions of long-wave instability but the absolute minimum of the neutral curve is supplied by the cellular mode. At $Gr_d = -500$ the long-wave mode is most dangerous ; the transition takes place at $Gr_d \cong -477$. Thus, the stability boundary on the plane (Gr_d, Gr) (Fig. 9) is associated with the cellular mode in the region $Gr_d > -477$ and with the long-wave mode when $Gr_d < -477$. Calculations show that in the region of large absolute negative values of Gr_d $(Gr_d < -1860)$ the reverse transition to the cellular form of instability takes place.

The picture of interaction between the long-wave and cellular modes of instability changes when the Schmidt number, Sc, increases. This is due to the fact

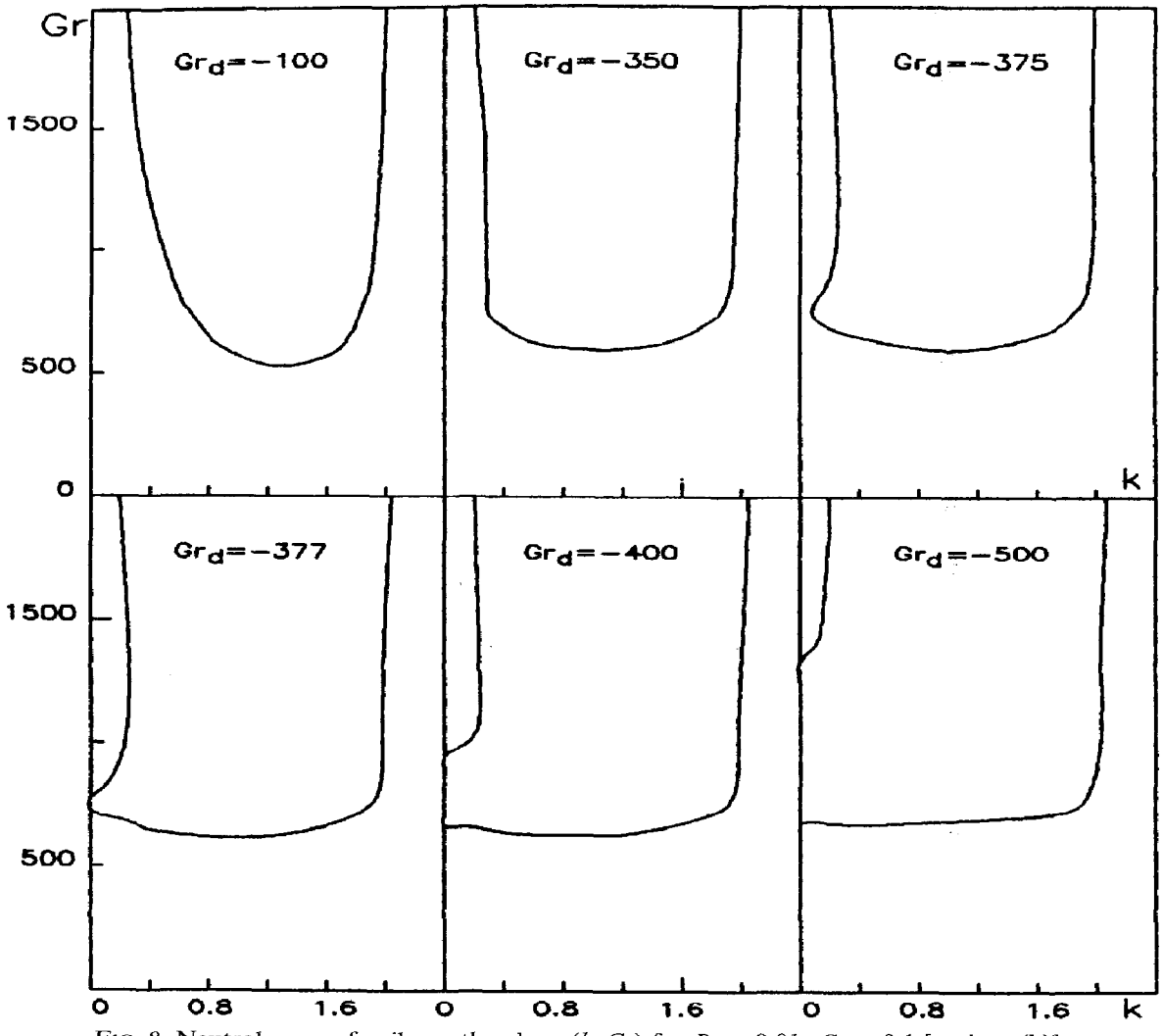

FIG. 8. Neutral curves family on the plane (k, Gr) for $Pr = 0.01$; $Sc = 0.1$ [variant (b)].

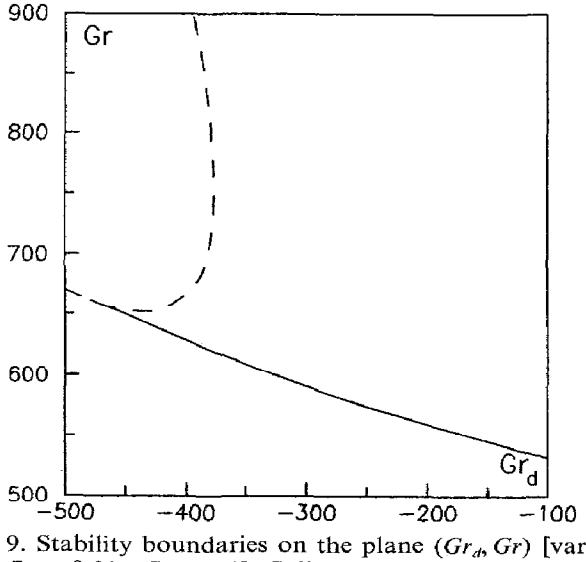

FIG. 9. Stability boundaries on the plane (Gr_d, Gr) [variant (b); $Pr = 0.01$; $Sc = 0.1$]. Solid curve, cellular instability boundary (results from minimization with respect to k). Dashed curve, instability boundary of long-wave mode determined by equation (41).

that, when the long-wave instability first appears at some negative value of Gr_d, it becomes most unstable at once. An example of such a situation is presented in Figs. 10 and 11, where a family of neutral curves $Gr(k)$ and stability boundaries on the plane (Gr_d, Gr) are shown for $Sc = 0.5$. The neutral curve corresponding to $Gr_d = -75$ has a minimum and determines the instability of pure cellular type. As $|Gr_d|$ increases, the neutral curve minimum becomes lower and shifts to the side of small values of k. According to formula (41) at $Gr_d = -75.3$ the region of long-wave instability arises which is adjacent to the ordinate axis. When $Gr_d < -75.3$, the long-wave mode is most dangerous because it corresponds to lower (with respect to the cellular mode) values of the critical Grashof number, Gr. A further increase in $|Gr_d|$ leads to the unification of the instability regions on the plane (Gr_d, Gr) and to the disappearance of the cellular mode (at $Gr_d \approx -78.4$). In the region of large absolute negative values of Gr_d the minimum of the neutral curve again corresponds to $k_m \neq 0$, so the cellular

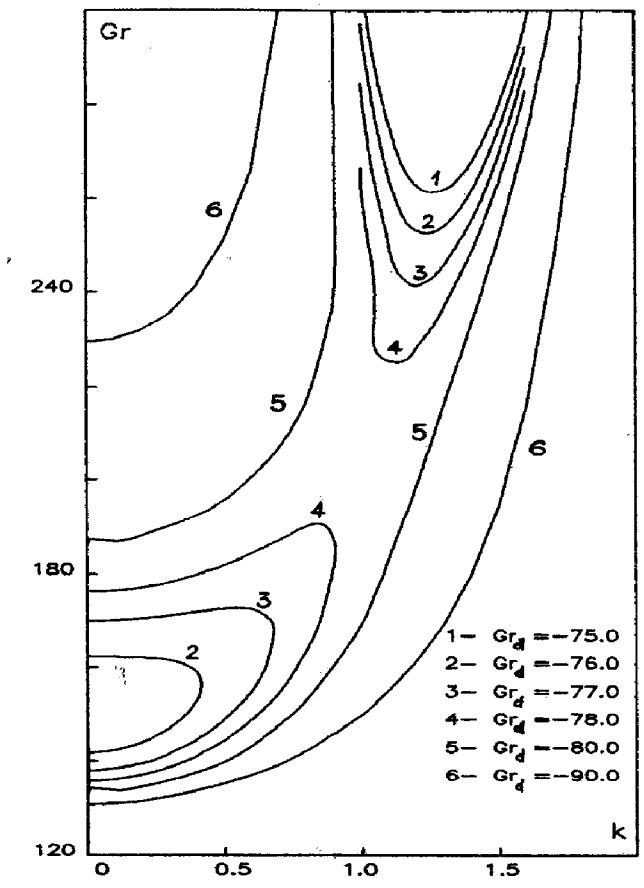

FIG. 10. Family of neutral curves for $Pr = 0.01$; $Sc = 0.5$ [variant (b)].

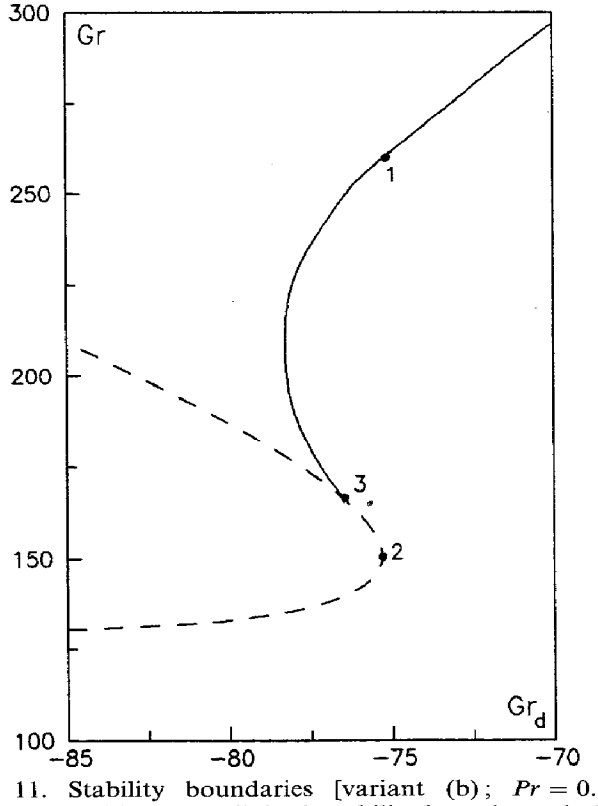

FIG. 11. Stability boundaries [variant (b); $Pr = 0.01$; $Sc = 0.5$]. Solid curve, cellular instability boundary; dashed curve, long-wave instability boundary.

mode again becomes most dangerous (when $Gr_d < -365.6$).

The stability boundaries on the plane (Gr_d, Gr) in the region of transition from the cellular to the long-wave mode are shown in Fig. 11. By determining the threshold value of the critical number Gr at a fixed Gr_d, it can be seen that non-singularity takes place. In the region $Gr_d > -75.3$, instability is connected with the cellular mode, whereas for $Gr_d < -75.3$ with the long-wave mode. At the point $Gr_d = -75.3$ the jump-like changes of the critical Grashof number and critical wavenumber take place (transition between points 1 and 2 in Fig. 11). On the other hand, if one determines the threshold value of Gr_d at a fixed Gr, then the picture is as follows: when $Gr < 65.21/Sc = -130.4$, the flow is stable [see equation (41)]. Within the range $130.4 < Gr < 164$, the instability caused by the long-wave mode (the right boundary of the interval is determined by the position of point 3 in Fig. 11). When $Gr > 164$, the instability is of cellular character.

In Fig. 12 the summary family of stability curves on the plane (Gr_d, Gr) for few different values of Schmidt number is presented for variant (b). As compared with variant (a) (Fig. 4), one can mark rather a sharper stabilization of hydrodynamical mode in the region of positive Gr_d values as the Schmidt number increases, and also the existence of specific competition between long-wave and cellular disturbances in the region of negative Gr_d values.

In the case of variant (c), when both boundaries are impermeable and thermally insulated, there exist only quantitative distinctions from variant (b). In particular, both above-described 'scenarios' of interaction between cellular and long-wave modes are preserved. In Fig. 13 the stability boundaries on the plane (Gr_d, Gr) are presented, whereas in Fig. 14 the dependence of the critical wavenumber on Gr_d is shown. As is seen at a fixed Schmidt number, Sc, there exists an interval of the Gr_d values inside of which the long-wave mode is most dangerous. The upper and lower boundaries of this interval are shown as functions of Sc in Fig. 15 (curves 1 and 2, respectively). Thus, the region of long-wave instability on the plane of (Gr_d, Sc) is just confined between these two curves. Note that these regions for variants (b) and (c) practically coincide.

We do not present here the results of studying the form of neutral disturbances as eigenfunctions of spectral amplitude problem (20), (21). Note only that irrespective of the physical nature of the instability mechanism in the parameter region studied the neutral disturbances have the form of a system of vortices which is periodical along the x-axis.

10. CONCLUSION

The linear stability of steady plane-parallel binary mixture advective flow in a horizontal layer under the

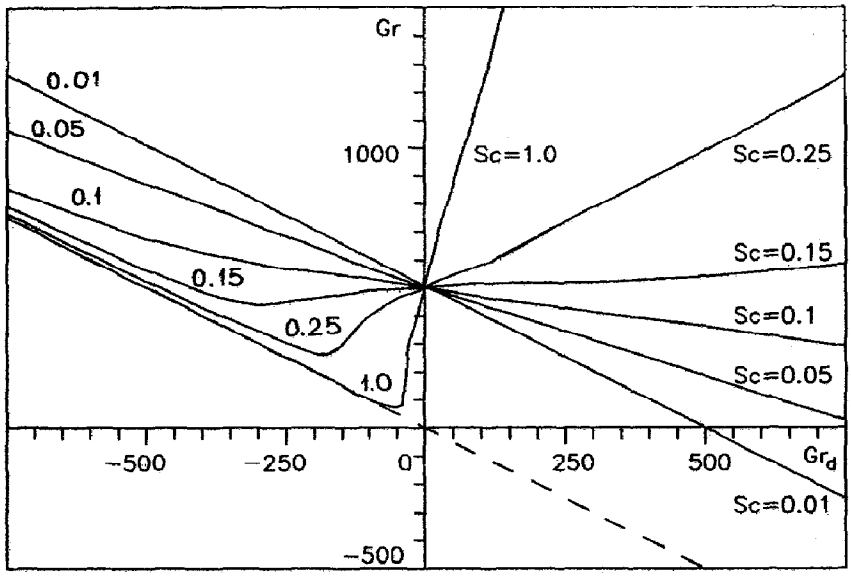

FIG. 12. Stability curves on the plane (Gr_d, Gr) [$Pr = 0.01$; variant (b)].

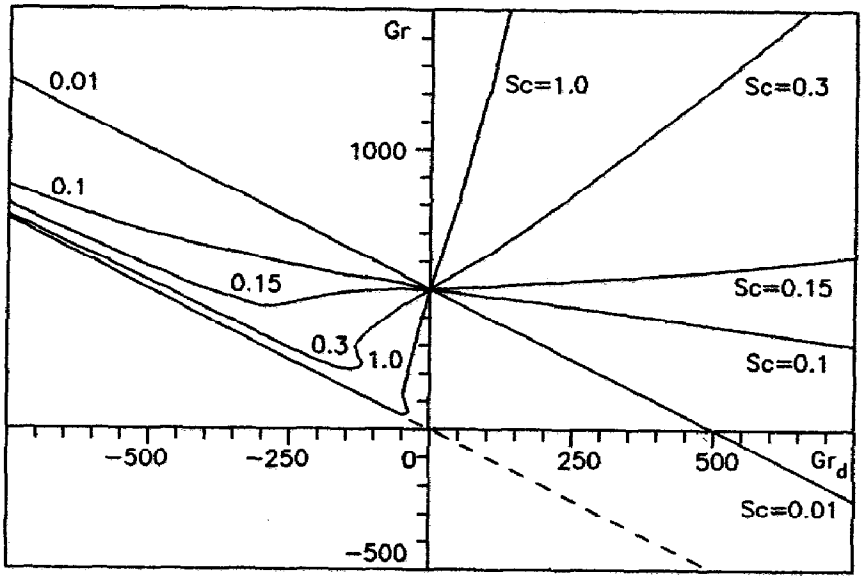

FIG. 13. Stability curves on the plane (Gr_d, Gr) [$Pr = 0.01$; variant (c)].

action of longitudinal temperature and concentration gradients is investigated. Three variants of boundary conditions on rigid boundaries are considered: (a) constant temperature and concentration gradients are maintained; (b) temperature gradient is maintained whereas the boundaries are impermeable; and (c) both boundaries are impermeable and thermally insulated. The spectral amplitude problem for small 2D disturbances is formulated. The stability boundaries for the case of mechanical equilibrium are determined. For the cases of variants (b) and (c) the stability boundaries for long-wave disturbances are determined analytically. The complete spectral amplitude problem is solved numerically for $Pr = 0.01$ and $Sc \geqslant Pr$ (liquid metal or semiconductor containing an admixture). The stability boundaries and characteristics of neutral disturbances are determined. It is shown that in all the cases considered the instability mechanism varies with the parameters, i.e. the transition from hydrodynamical to thermo-concentrational mechanism.

Acknowledgements—We would like to thank Dr D. V. Lyubimov for many fruitful discussions of the results of

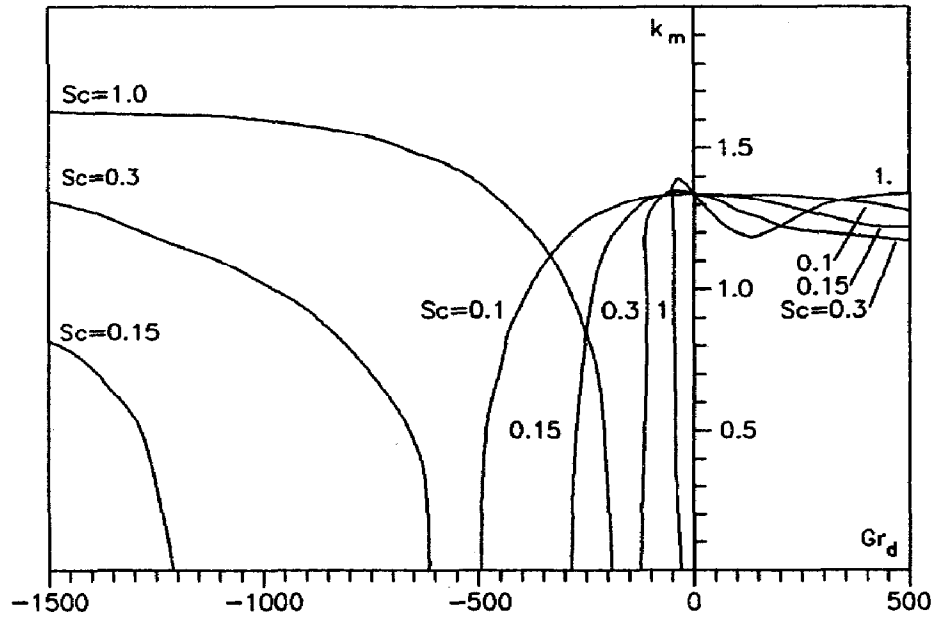

FIG. 14. Critical wavenumber k_m vs Gr_d [$Pr = 0.01$; variant (c)].

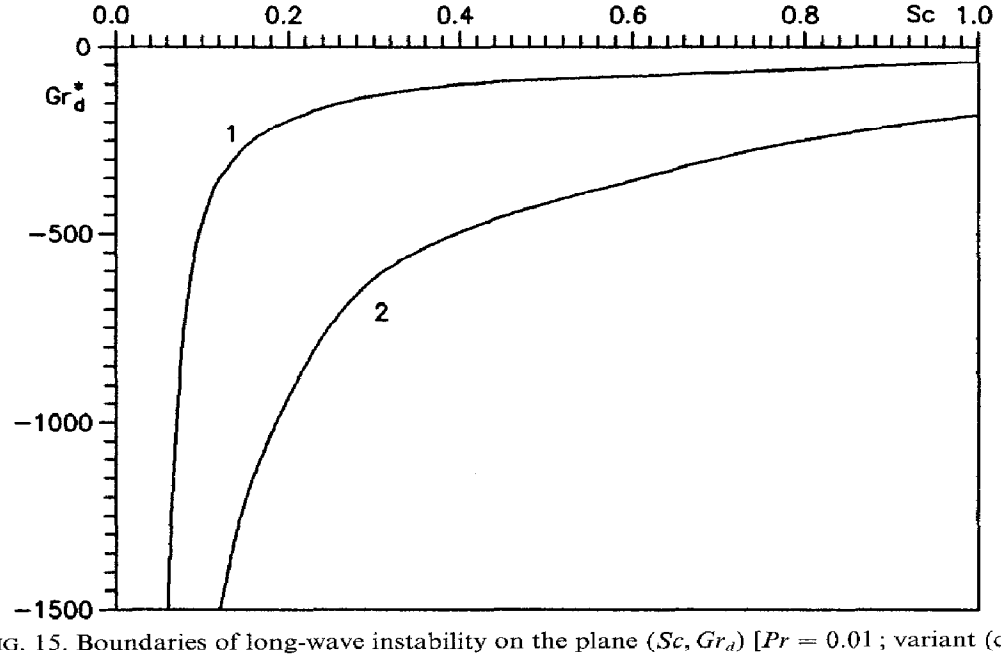

FIG. 15. Boundaries of long-wave instability on the plane (Sc, Gr_d) [$Pr = 0.01$; variant (c)].

this work. The work was supported, in part, by a Soros Foundation Grant awarded by the American Physical Society.

REFERENCES

1. G. Z. Gershuni, E. M. Zhukhovitsky and A. A. Nepomnyashchy, *Stability of Convective Flows*. Izd. Nauka, Moscow (1989).
2. G. Z. Gershuni, P. Laure, V. M. Myznikov, B. Roux and E. M. Zhukhovitsky, On stability of plane-parallel advective flows in long horizontal layers, *Micrograv. Quart.* **2**, 141–151 (1992).
3. V. S. Avduevsky, I. V. Barmin, S. D. Grishin, L. V. Leskov, A. P. Petrov, V. I. Polezhaev and V. V. Savichev, *The Problems of Industry in Space*. Izd. Mash., Moscow (1980).
4. V. I. Polezhaev, M. S. Bello, N. A. Verezub, K. G. Dubovik, A. P. Lebedev, S. A. Nikitin, D. S. Pavlovsky and A. I. Fedyushkin, *Convective Processes in Weightlessness*. Izd. Nauka, Moscow (1991).
5. D. S. Pavlovsky, Solution of convective stability problems for multicomponent fluids, Preprint no. 416 of the Institute for Problems in Mechanics, Moscow (1989).
6. K. G. Dubovik, D. S. Pavlovsky, V. I. Polezhaev and A. I. Fedyushkin, Convective processes by HTSC-monocrystal growth, Preprint No. 434 of the Institute for Problems in Mechanics, Moscow (1990).
7. V. M. Myznikov, On instability mechanisms of binary mixture advective flow, *Hydromechanics and Heat/Mass*

Transfer in Microgravity Symp., Perm, Moscow, pp. 543–547. Gordon & Breach (1992).
8. G. Z. Gershuni and E. M. Zhukhovitsky, *Convective Stability of Incompressible Fluid.* Izd. Nauka, Moscow (1972).
9. R. V. Birikh, On thermocapillary convection in horizontal fluid layer, *J. Appl. Mech. Technol. Phys.* **3**, 67–72 (1966).
10. M. A. Goldshtik and V. N. Stern, *Hydrodynamic Stability and Turbulence.* Izd. Nauka, Novosibirsk (1977).